

64435 HETEROGENEOUS IMPACT MELT, PARTLY GLASS-COATED 1079 g

INTRODUCTION: 64435 is a coherent, very light gray, heterogeneous impact melt that contains abundant clasts of pristine ferroan anorthosite (Fig. 1). A glass coat is present on the surface of the rock, which was partly buried in the lunar regolith. These protected surfaces are devoid of zap pits whereas the surfaces that were exposed on the Moon have many zap pits. The sample was collected from the northeast wall of a small, subdued crater on the northeast side of Stone Mountain. The lunar orientation is known.

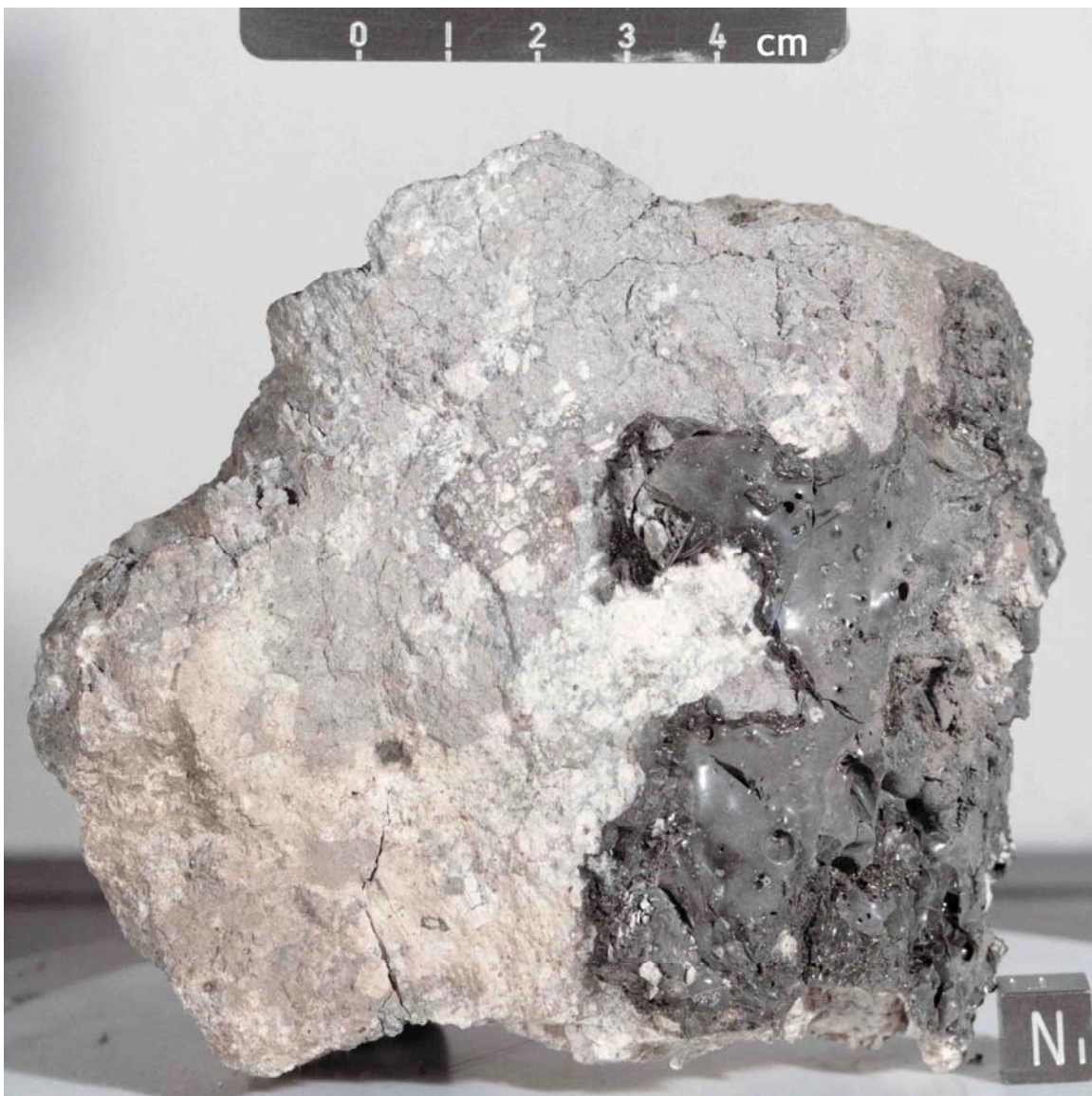


FIGURE 1. S-72-39674.

PETROLOGY: 64435 consists of three main lithologies: 1) a light gray matrix of heterogeneous, plagioclase-rich impact melt, 2) anorthosite clasts and 3) a partial coating of dark glass. The Apollo 16 Lunar Sample Information Catalog (1972) and Mason (unpublished data pack information) provide petrographic descriptions.

The light gray matrix accounts for ~80% of the rock and is somewhat variable in texture, often with sharp contacts between the different textures. Portions of the matrix have subhedral laths of plagioclase (An_{95-100} , up to ~0.5 mm) suspended in a very fine-grained, clast-rich melt (Fig. 2). Most of the laths and clasts have fine-grained reaction rims with the matrix. A flow alignment is often obvious. Shock effects range from moderate in the clasts to absent in the laths. Other portions of the gray matrix are more clastic with anhedral, lightly to moderately shocked clasts of plagioclase, pyroxene, and minor olivine, cemented together by a small amount of interstitial mesostasis. Very small (<5 μm) mafics and opaques with a melt texture are concentrated in these interstices. Still other portions of the gray matrix have a variolitic to basaltic texture. Angular clasts of basaltic impact melt, metal, troilite, ilmenite and ulvospinel (?) are inhomogeneously distributed throughout the rock. A few small brown glass veins also cut the matrix.

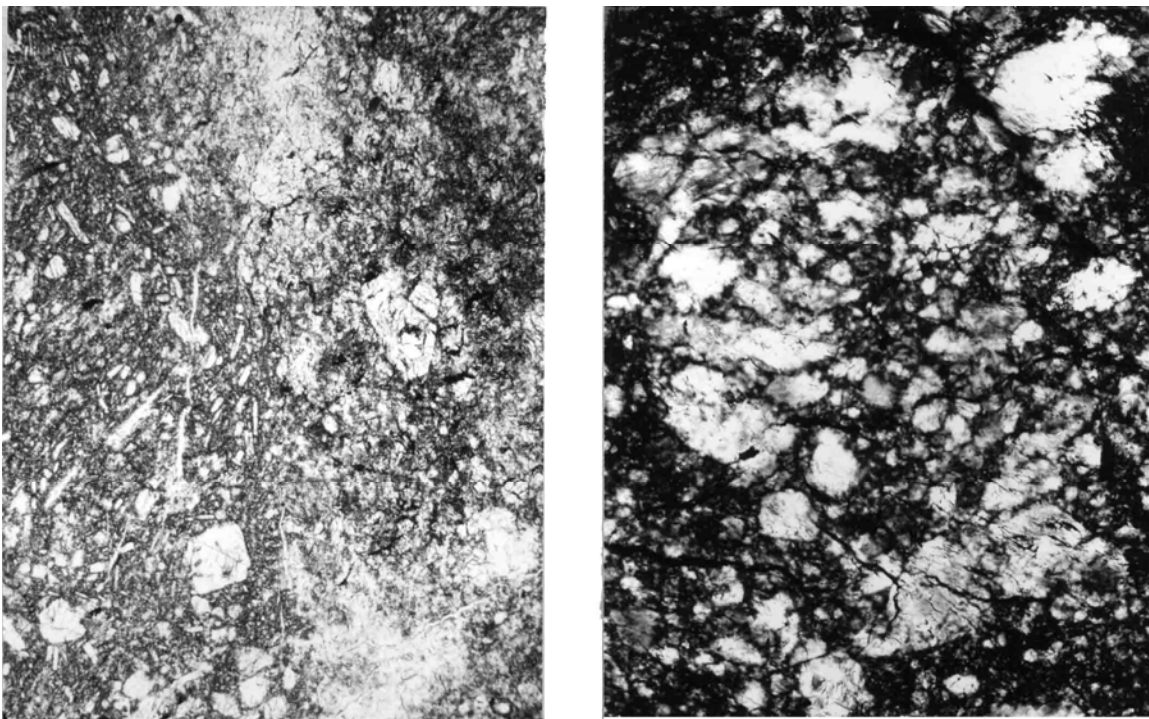


FIGURE 2. a) 64435,8, matrix, ppl. Width 2 mm.
b) 64435,73, anorthosite clast, ppl. Width 2 mm.

The anorthosite clasts consist of ~98% plagioclase (An_{95-100}) with minor pyroxene, olivine and metal (Fig. 2). Pre-cataclasis grain size was >0.5 mm. A single grain of augite had the composition $Wo_{44}En_{36}$ (Mason, unpublished), similar to those in other ferroan anorthosites. Hewins and Goldstein (1975a) find the metal in the anorthosite

clasts to have Co too high to be of meteoritic origin (Fig. 3) and compositionally similar to the metal in pristine anorthosite 60015. No maskelynite was observed in any of the anorthosite clasts.

The dark glass coating is present only on the surface of the rock that was buried on the lunar surface. It is somewhat vesicular and clast-rich near the rock-glass contact. Away from the rock the glass is isotropic, showing no signs of devitrification. Metal in the glass contains ~30% Ni (Cisowski et al., 1976).

CHEMISTRY: Laul et al. (1974) provide major and trace element analyses of an anorthosite chip, the gray matrix and the glass coat. Major and trace element data on the matrix are also given by Hubbard et al. (1974) and S.R. Taylor et al. (1974). Mason (unpublished data pack information) determined major elements on a chip of matrix fused to a glass and on fragments of the glass coat, by electron microprobe. Moore et al. (1973), Cripe and Moore (1974) and Moore and Lewis (1976) report total C, N and S on a matrix chip. Nunes et al. (1974, 1977) provide U-Th-Pb data on the matrix.

The gray matrix is aluminous (Table 1) with its rare earths and other trace elements dominated by a small amount of KREEP (Fig. 4). A chip from the large area of anorthosite on the W surface of the rock is nearly pure plagioclase (Table 1) and has rare earth element abundances similar to other pristine anorthosites (Fig. 4). The lack of KREEP contamination and the low levels of siderophiles (Co 1.3 ppm) indicate that the anorthosite portion of this rock is chemically pristine. The glass coat is significantly different in both major and trace elements from the rest of 64435 and from the local soils. It is highly enriched in siderophiles and contains a significant KREEP component (Table 1, Fig. 4).

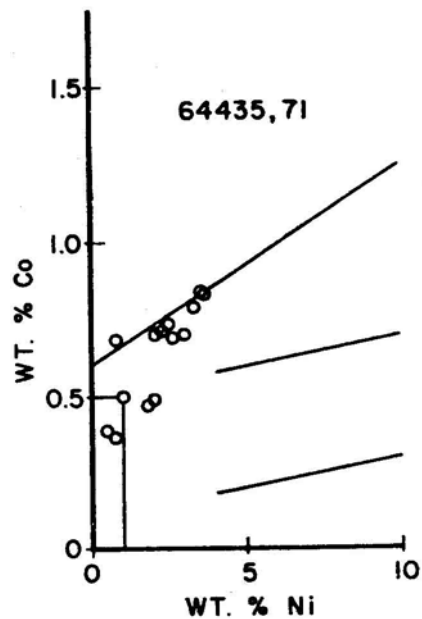


FIGURE 3. Metals in anorthosite clasts, from Hewins and Goldstein (1975a).

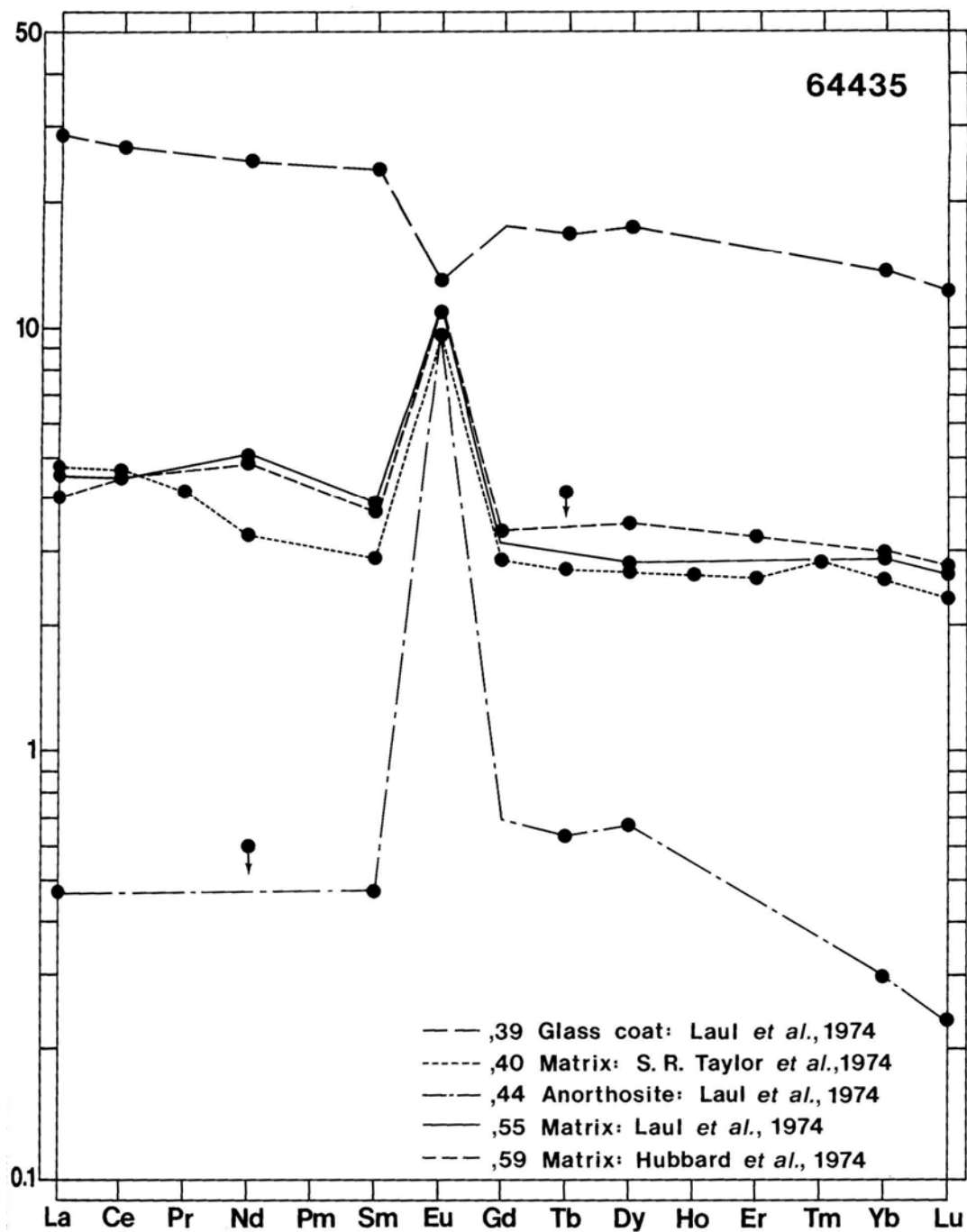


FIGURE 4. Rare earths.

From light gas (H₂O, CO₂, N₂, CO, SO₂) releases at different temperatures, Gibson and Moore (1975) find evidence for possible carbonate phases in the matrix (Fig. 5). An anorthosite clast does not contain these possibly carbonate phases. Gibson and Andrawes (1978) find that nitrogen and a trace of methane are the only gases given off when chips

of matrix and of an anorthosite clast are crushed under 25 tons of pressure.

TABLE 1. Summary chemistry of 64435 lithologies.

	<u>Matrix</u>	<u>Anorthosite clasts</u>	<u>Glass coat</u>
SiO ₂	44.5		
TiO ₂	0.19	<0.1	0.5
Al ₂ O ₃	31.1	35.5	24.5
Cr ₂ O ₃	0.069	0.0083	0.170
FeO	3.18	0.61	8.0
MnO	0.04	0.011	0.105
MgO	3.3		8.0
CaO	17.3	19.0	13.3
Na ₂ O	0.34	0.29	0.55
K ₂ O	0.025	0.025	0.086
P ₂ O ₅	0.03		
Sr	154		
La	1.5	0.16	9.6
Lu	0.08	0.008	0.43
Rb	0.5		
Sc	6	0.9	6.9
Ni	56		1800
Co	17	1.3	100
Ir ppb			50
Au ppb			30
C	46		
N	56		
S	330		
Zn			
Cu			

oxides in wt%; others in ppm except as noted.

RADIOGENIC ISOTOPES AND GEOCHRONOLOGY: Nunes et al. (1974, 1977) and Rosholt (1974) provide U-Th-Pb isotopic data on the gray matrix. This lithology contains excess Pb relative to U which is isotopically very similar to, but much less abundant than, the Pb in 66095. The excess Pb is characterized by a high ²⁰⁷Pb/²⁰⁶Pb ratio (1.25) and was apparently produced in a U-rich reservoir very early in lunar history. A two-stage model age of 3.73 - 4.0 b.y. for the introduction of the excess Pb into the rock and a three-stage model age of 4.42 to 4.65 b.y. for the production of the U-rich reservoir were calculated by Nunes et al. (1977).

A measured ⁸⁷Sr/⁸⁶Sr ratio of 0.69978 ± 6 for a matrix chip was reported by Wiesmann

and Hubbard (1975).

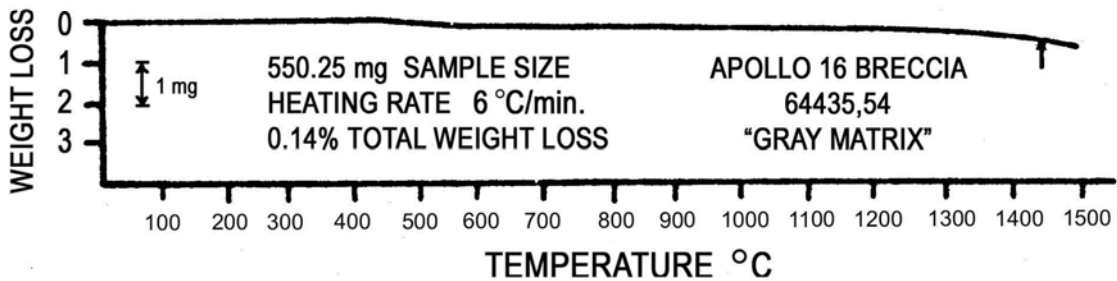
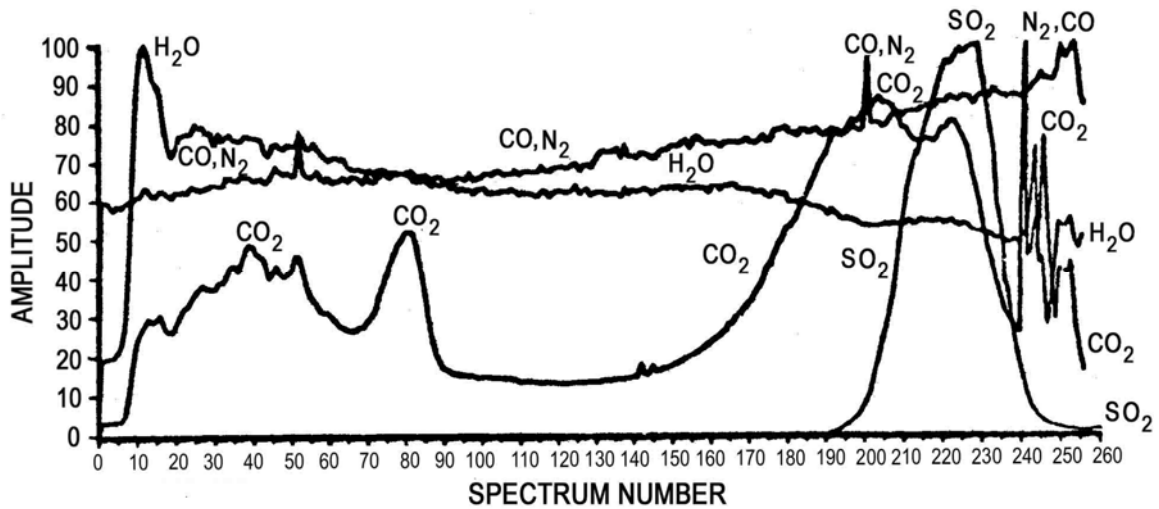
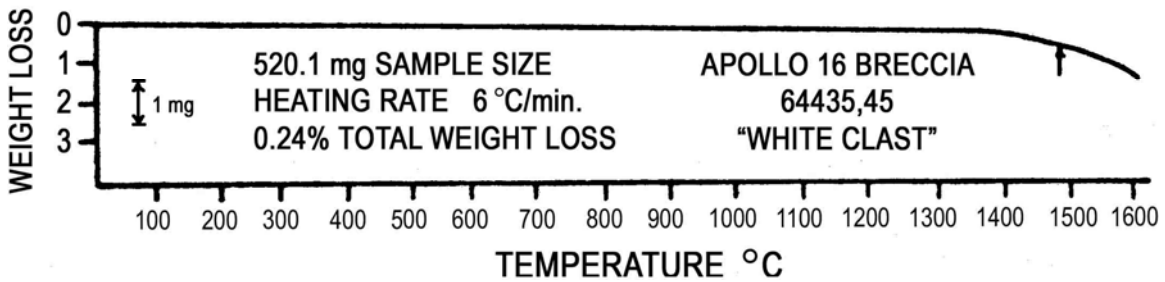
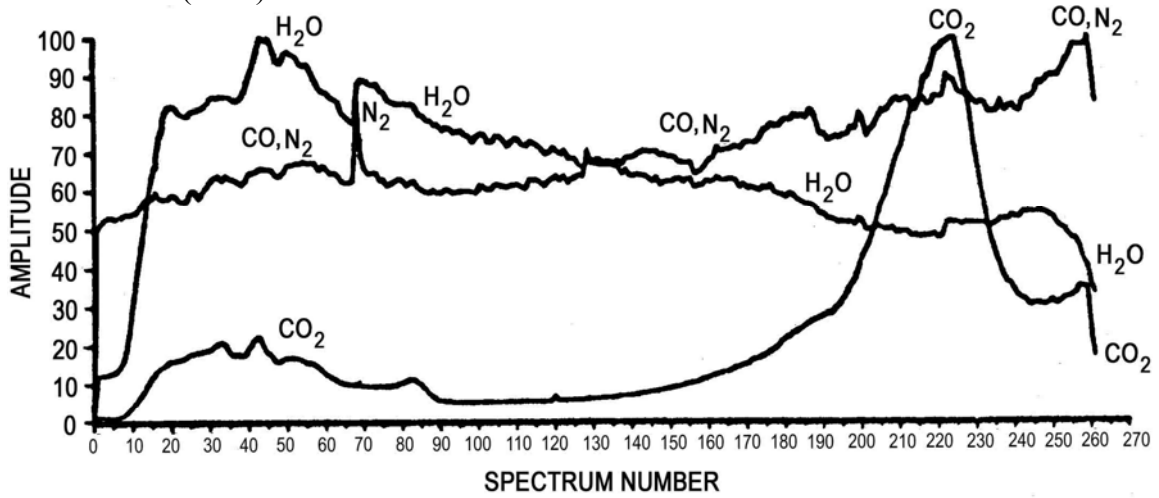


FIGURE 5. Gas release profiles, Gibson and Moore (1975).

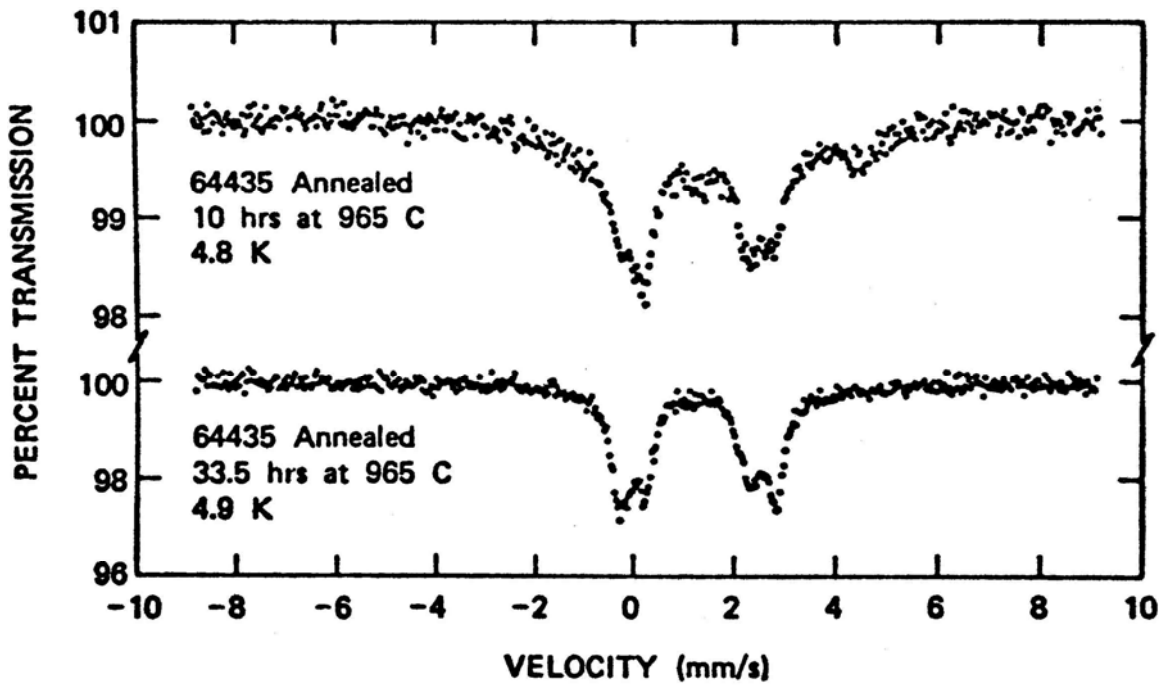
RARE GAS/EXPOSURE AGES: Bogard et al. (1973) report He, Ne, Ar and Kr isotopic data for an interior matrix chip. From these data Bogard and Gibson (1975) calculate ^{21}Ne and ^{38}Ar exposure ages of 0.6 and 0.7 m.y. (both ± 0.3 m.y.), respectively. Bhandari et al. (1976) give an “insolation age” of 0.5 m.y. from galactic cosmic ray tracked a crater-count exposure age of 0.2 - 2 m.y. for an exterior matrix chip. From ^{26}Al data on this same exterior chip, Bhandari (1977) calculates an exposure age of $0.5 + 0.1$ m.y. Fruchter et al. (1978) analyzed an interior matrix chip with >2 cm shielding on all sides and report ^{26}Al and ^{53}Mn exposure ages of 1.3 and 1.7 m.y. (both ± 0.3 m.y.) respectively.

PHYSICAL PROPERTIES: Basic and remanent magnetic properties of the gray matrix indicate 0.096 wt% metal and no significant residue of NRM after 150 Oe.rms demagnetization (Nagata et al., 1974). Cisowski et al. (1976) provide magnetic data on a split of the glass coat. The field acquired by the glass is similar to that presently observed at the Apollo 16 site. Schwerer and Nagata (1976) determined the size distribution of metallic particles in the range 0.003 - 0.015 μm (30-150 \AA) by magnetic granulometry on a matrix chip. The mean grain size of fine-grained metal in the matrix is 62 \AA .

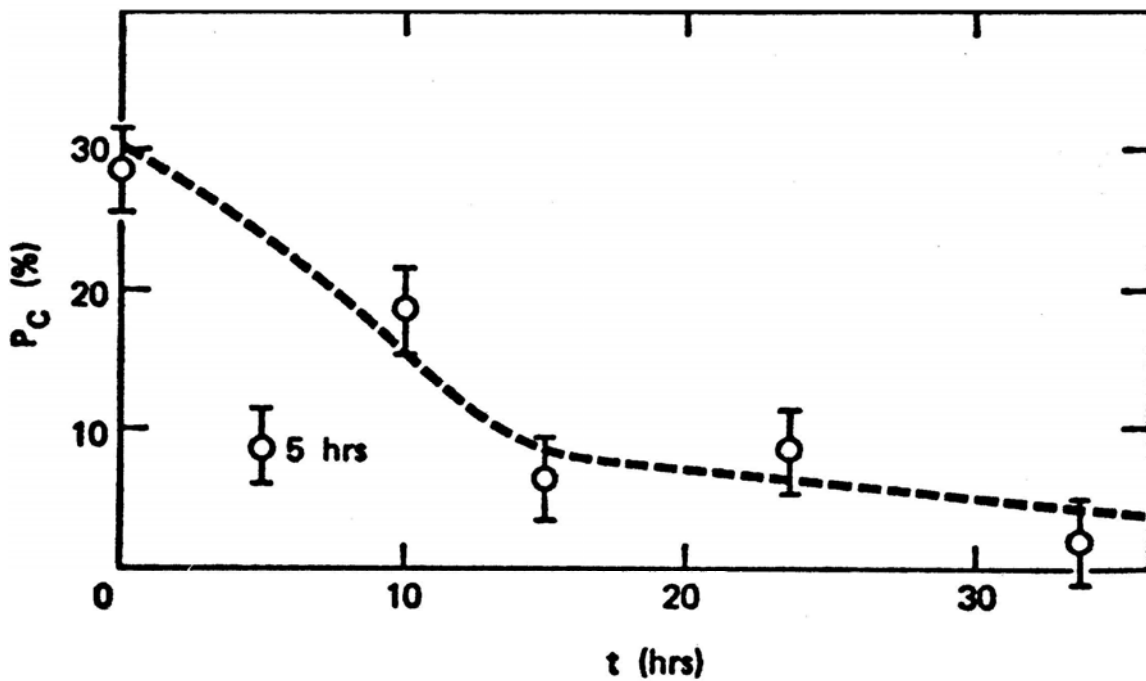
Huffman et al. (1974) report the phase distributions of iron and the metallic/ferrous iron ratio in the gray matrix as determined by Mossbauer and magnetic analyses. Huffman and Dunmyre (1975) provide data on superparamagnetic clusters of ferrous iron spins in matrix olivines and the results of heat treatments on these clusters. With increasing time of subsolidus annealing, the percentage of total iron in these clusters progressively decreases (Fig. 6).

Charette and Adams (1977) give spectral reflectance data for an interior matrix chip (Fig. 7).

PROCESSING AND SUBDIVISIONS: In 1973, 64435 was cut into three main pieces, including a slab (Figs. 8, 9, 10). The slab and the smaller butt end (,12) were extensively subdivided for allocations. Most of the slab samples consist of matrix (Fig. 9). The anorthosite clasts studied by Hewins and Goldstein (1975a) are in thin sections made from slab split ,22. The anorthosite chip (,44) analyzed by Laul et al. (1974) is from the area of massive anorthosite seen on the W and N surfaces (Fig. 1).



Liquid-helium spectra of 64435 after 10 and 33.5 hr of annealing at 965°C.



Superparamagnetic cluster percentage as a function of annealing time at 965°C for sample 64435.

FIGURE 6. From Huffman Dunmyre (1975).

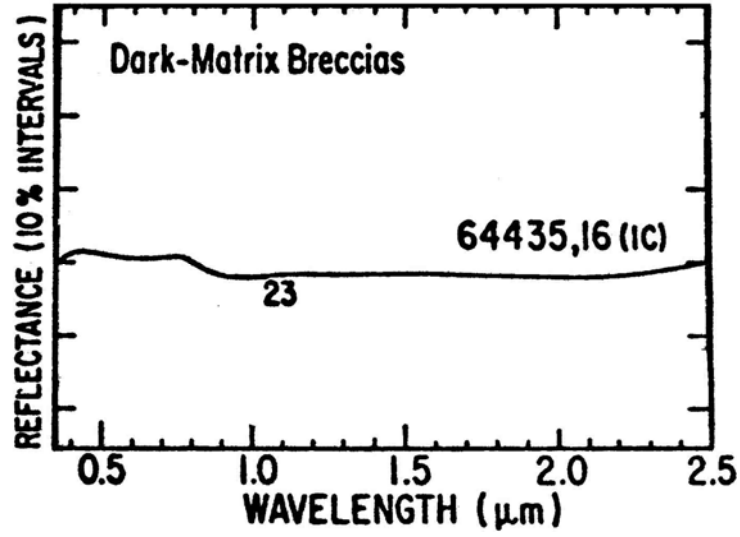


FIGURE 7. From Charette and Adams (1977).

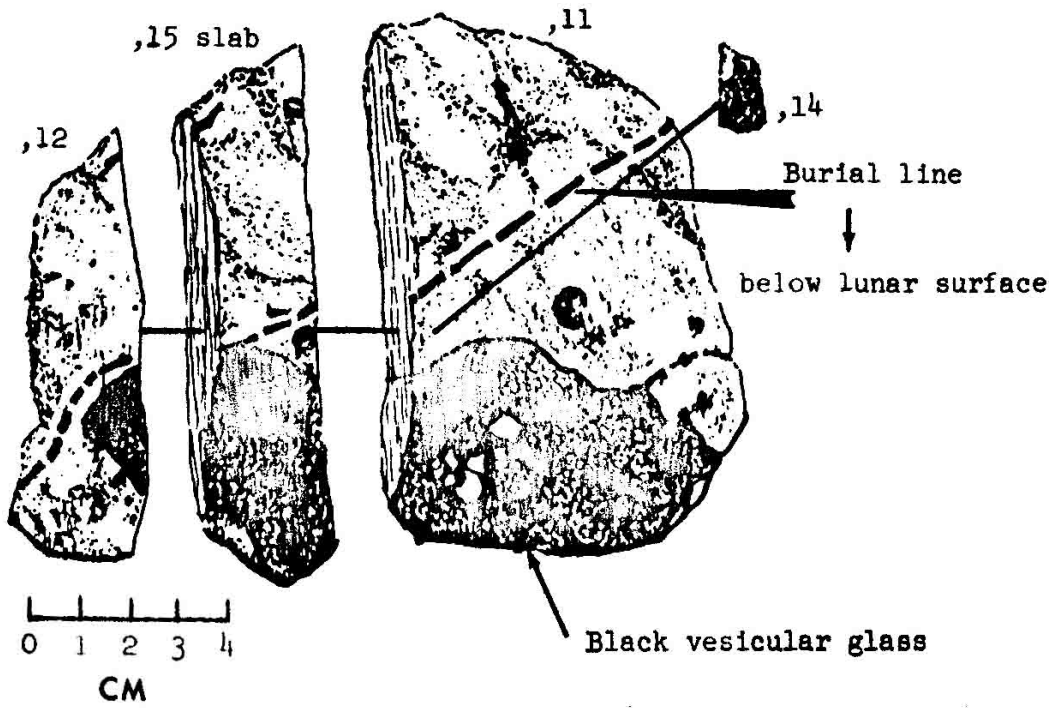


FIGURE 8. Cutting sketch.



FIGURE 9. Slab face, prior to subdivisions. S-73-16140.

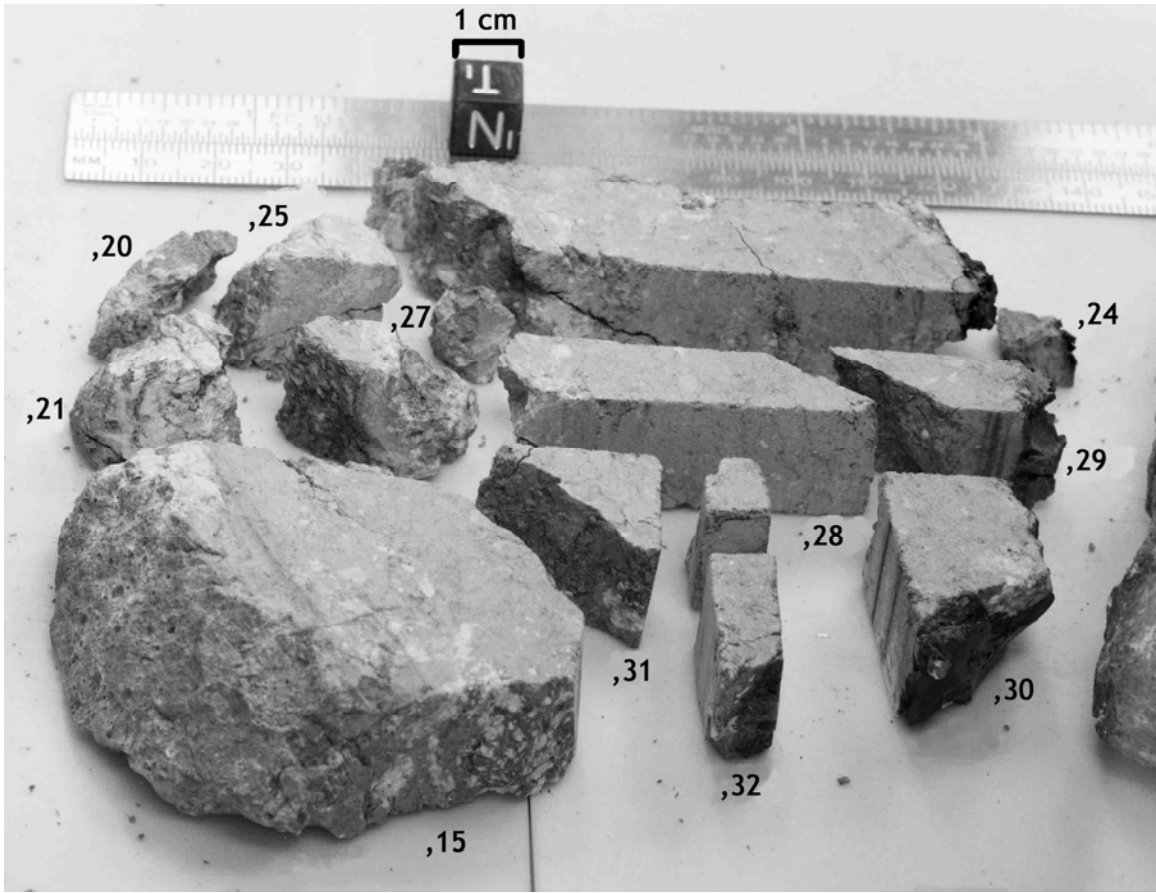


FIGURE 10. Slab subdivisions. S-73-17794.